Local Similarity Relationships of Non-Dimensional Wind and Temperature Gradient in the Tower-Layer Atmosphere over Beijing City[①]

Al-Jiboori M. H.[②], Xu Yumao (徐玉貌) and Qian Yongfu (钱永甫)

Department of Atmospheric Sciences, Nanjing University, Nanjing 210093

(Received January 24, 2000; revised April 13, 2000)

ABSTRACT

Micrometeorological data for wind and temperature from a 325 m high tower in Beijing City are analyzed by use of local similarity theory. Non-dimensional wind and temperature gradients, Φ_m and Φ_θ, are determined by three techniques called, respectively, eddy-correlation, mean profiles and inertia-subrange cospectra (ISC) method for a wide range of atmospheric stratification from unstable to stable conditions. Average dissipation rate Φ_ε of turbulent kinetic energy (TKE) is evaluated from u-spectrum, as a quantity required in the last technique. Ratio of the eddy transfer coefficients, $\alpha (= K_\theta / K_m)$, is calculated from Φ_m and Φ_θ estimations. The results from various techniques are compared with each other and with some available empirical results in the tower-layer. It is shown that the empirical relationships determined by mean profiles and ISC methods in the tower-layer turbulence are in agreement with each other and with some other results.

Key words: Local similarity, Non-dimensional gradients of wind and temperature, Dissipation rate, Ratio of eddy diffusivities, Spectra and Cospectra

1. Introduction

The local similarity theory is one of the powerful tools of similarity theory in the analysis of turbulence flow in the atmospheric boundary layer (ABL). This theory provides a set of empirical relationships to describe the meteorological parameters in the tower-layer atmosphere. These relationships can be expressed as a function of stability parameter, $\zeta_1 (= z / L_1)$, where z is the height and L_1 the local Monin-Obukhov length. Monin-Obukhov similarity has been applied to the surface layer (e.g. Monin and Obukhov, 1954; Businger et al., 1971), while local similarity theory is limited to the lower level of the ABL (e.g. Nieuwstadt, 1984; Sorbjan, 1986a,b; Zhang et al., 1991; Hu and Zhang, 1993; Xu et al., 1997; Al-Jiboori et al., 2000).

Most previous studies analyzed the turbulence characteristics in the tower-layer and pointed out that dimensionless standard deviations, gradient fluxes and dissipation rates for velocity and temperature variance are functions of ζ_1. The local similarity proposed first by Nieuwstadt (1984) was applied to describing turbulence characteristics over meteorological mast in the stable boundary layer. Based on the data from the same tower used in the present study, Zhang et al. (1991) found that the dimensionless variable groups σ_i / u_{*1} are functions of (z / L_1) $(i = 1, 2, 3)$ under unstable conditions. Xu et al. (1997) showed that the

①Supported by the National Natural Science Foundation of China under Grant No.49735170.

②Ph. D. student in Nanjing University at present.

turbulence structure on meteorological towers in Nanjing City and its suburb could be ordered well by local similarity scales u_{*l}, space T_{*l}, space L_l, under stable and unstable conditions.

Most researchers have described the turbulent exchange processes between land surface and atmosphere as well as ocean and atmosphere in the ABL by using mean profile techniques. Flux-gradient relationships are essential for the synthesizing of turbulent fluxes of momentum and heat, and the predicting of diffusion of pollutants. Unfortunately, there are different forms and constants suggested for the functional representation of non-dimensional gradients, so that it is of interest to find the suitable and the reasonable technique and formulae through some comparison.

In the present paper, we focus on the determining of dimensionless functions of momentum and heat flux under a wide range of stratification conditions in the framework of local similarity theory in terms of three techniques, which adopt direct covariance (eddy correlation), mean wind and temperature profiles and inertia-subrange cospectra techniques, by use of tower-layer data over Beijing City. These methods are used to derive some universal expressions for the dissipation rates, wind shear and heat flux with ζ_l, variation of ratio of eddy coefficients as well as the spectral characteristics of turbulence. The results are compared with each other and then checked with well-defined results in the literature.

The mean wind and temperature profiles normalized with local velocity scale u_{*l} and temperature scale T_{*l}, respectively, should be the functions of either z/L_l or z/L'_l

$$\frac{kz}{u_{*l}}\frac{\partial \overline{U}}{\partial z} = \Phi_m \ , \tag{1}$$

$$\frac{kz}{T_{*l}}\frac{\partial \overline{T}}{\partial z} = \Phi_h \ . \tag{2}$$

where overbar is a time average, in this paper, the hourly average is taken, and the subscript 'l' denotes local values, the other relevant local parameters and formulations are listed below as those used by Nieuwstadt (1984) and Xu et al. (1997)

$\overline{U}$ mean horizontal wind speed,

$\overline{T}$ mean temperature,

L_l Monin-Obukhov length$= -\dfrac{\overline{T}u_{*}^{3}}{kg\overline{w'T'}}$,

L'_l the length defined by $\dfrac{u_{*}\dfrac{\partial \overline{U}}{\partial z}}{gk\dfrac{\partial \overline{T}}{\partial z}}$.

u, v, w, T the fluctuation values of velocity and temperature,

k Von Karman constant $= 0.4$,

g acceleration due to gravity.

2. Techniques

Non-dimensional wind and temperature gradients, Φ_m and Φ_h, may be computed by either so-called "direct" or "indirect" method. The former involves two techniques, while the latter has one, all of them will be explained, respectively below.

2.1 *Eddy–correlation technique*

Φ_m and Φ_h can be obtained by solving (1) and (2) in terms of local scales of velocity and temperature, and gradients of wind speed and temperature, respectively. The outputs of sonic anemometer can be applied to the calculation of local scales of velocity and temperature by

$$u_{*1}^2 = -\overline{u'w'} , \tag{3}$$

$$T_{*1} = -\frac{\overline{w'T'}}{u_{*1}} . \tag{4}$$

The wind and temperature gradients, $\partial\overline{U}/\partial z$ and $\partial\overline{T}/\partial z$, can be directly computed by using a differential approximation for the tower level data.

2.2 *Mean profile technique*

It is based on measurements of mean profiles of wind speed $\overline{U}$ and temperature $\overline{T}$ in the tower–layer atmosphere. As the above techniques, the non–dimensional gradients of Φ_m and Φ_h can also be described by (1) and (2) respectively, the mean wind and temperature gradients were estimated as the basic set of computations Φ_m and Φ_h. According to local similarity (e.g. Al–Jiboori et al., 1999 and Sugita et al., 1995), the fluxes u_{*1} and T_{*1} between successive two levels can be calculated by the following expressions:

$$u_{*1} = k(\overline{U}_{i+1} - \overline{U}_i)/[\ln(\frac{z_{i+1}}{z_i}) - \Delta\Psi_m] , \tag{5}$$

$$T_{*1} = k(\overline{T}_{i+1} - \overline{T}_i)/[\ln(\frac{z_{i+1}}{z_i}) - \Delta\Psi_h] , \tag{6}$$

where

$$\Delta\Psi_m = \int_{z_i}^{z_{i+1}} \frac{1-\Phi_m}{\zeta'} \quad \text{and} \quad \Delta\Psi_h = \int_{z_i}^{z_{i+1}} \frac{1-\Phi_h}{\zeta'} \tag{7}$$

are variations of stability correction functions for momentum and heat, respectively, where ζ' is z/L'_1. In this method, the functions Φ_m and Φ_h are taken as functions of z/L'_1. The quantity L'_1 is related to L_1 by

$$L_1 = \frac{K_m}{K_h} L'_1 = \frac{L'_1}{\alpha} , \tag{8}$$

where K_m and K_h are turbulent transfer coefficients for momentum and heat, respectively, α is defined by

$$\alpha = \frac{K_h}{K_m} = \frac{\overline{w'T'}}{\overline{u'w'}} \frac{\partial\overline{U}/\partial z}{\partial\overline{T}/\partial z} . \tag{9}$$

In order to solve (5) and (6), we assumed initial values of functions $\Delta\Psi_m$ and $\Delta\Psi_h$, then the iteration method was used to minimize the percentage error.

2.3 *Inertia–subrange cospectra (ISC) method*

The indirect method, which is proposed by Wyngaard and Cote (1972), is based on the relationships of cospectra $C_{uw}(n)$ and $C_{wT}(n)$ to vertical gradient $\partial\overline{U}/\partial z$ and $\partial\overline{T}/\partial z$ given by the following expressions:

$$nC_{uw}(n) = -\left(\frac{z}{2\pi}\right)^{4/3}\beta\frac{\partial\overline{U}}{\partial z}\varepsilon^{1/3}f^{-4/3}, \tag{10}$$

$$nC_{wT}(n) = -\left(\frac{z}{2\pi}\right)^{4/3}\gamma\frac{\partial\overline{T}}{\partial z}\varepsilon^{1/3}f^{-4/3}, \tag{11}$$

where $f(=2\pi n/\overline{U})$ is dimensionless frequency, ε is a dissipation rate for TKE, β and γ are non-dimensional cospectral constants. Equations (10) and (11) can be solved by using (1) and (2) as well as the non-dimensional dissipation rate defined as follows:

$$\Phi_\varepsilon = \frac{kz\varepsilon}{u_{*1}^3}. \tag{12}$$

Substituting (1) and (2) into Equations (10) and (11) leads to the following equations:

$$\frac{nC_{uw}(n)}{u_{*1}^2} = -(2\pi k)^{-4/3}\beta\Phi_m\Phi_\varepsilon^{1/3}f^{-4/3}, \tag{13}$$

$$\frac{nC_{wT}(n)}{u_{*1}T_{*1}} = -(2\pi k)^{-4/3}\gamma\Phi_h\Phi_\varepsilon^{1/3}f^{-4/3}. \tag{14}$$

In fact, there are no detailed studies about the estimation of the constants ζ and γ except Wyngaard and Cote's paper (1972) (see Fig. 2). Although the combinations $\beta\Phi_m\Phi_\varepsilon^{1/3}$ and $\gamma\Phi_h\Phi_\varepsilon^{1/3}$ have been determined by some researchers directly from measurements of cospectra in the inertia-subrange (e.g. Kaimal et al., 1972; Roth and Oke, 1993).

We can get Φ_m and Φ_h by use of (13) and (14) and the cospectral constants given by Wyngaard and Cote (1972), where Φ_ε was calculated by the following way. The dissipation rate ε of TKE was firstly obtained from a regression of the spectral density of the longitudinal velocity in the inertia-subrange of slope '$-5/3$' power law

$$S_u(n) = \alpha_u\varepsilon^{2/3}(2\pi n/\overline{U})^{-5/3}, \tag{15}$$

where α_u is the Kolmogorov constant, taken as 0.55 (e.g. Antonia et al., 1979; Kaimal and Finnigan, 1994). Then, by replacing the natural frequency n with the non-dimensional frequency f and substituting (12) into (15), Equation (15) becomes

$$\frac{nS_u(n)}{u_{*1}^2} = \alpha_u(2\pi k)^{-2/3}\Phi_\varepsilon^{2/3}f^{-2/3}. \tag{16}$$

finally, Φ_ε was estimated by (16).

3. Site and data acquisition

The data came from a meteorological tower of 325 m height, located at straight north of Beijing City, 1 km away from Sanhuan Road. In the last two years many high buildings have been set up to the south of this Road 100 m away. The observation field around the tower is a relatively flat field, for planting wheat and short grass. There are several scattered observation rooms not higher than 4 m around the tower. The surface roughness lengths, z_0, were estimated by Yin and Hong (1999) by using the tower data, according to the wind directions (in degrees). The values of z_0 were 4.0 m for 0–90, 4.5 m for 90–180 and 3.1 m for 270–360,

respectively.

The synchro-measurement for atmospheric pollutants (O_3, No_x, Co) and meteorological elements (wind, temperature, humidity) in the tower layer was conducted during the period of October 7 to November 6, 1998. Two kinds of meteorological data sets were collected to do this study. The first data-set includes an hourly mean wind speed and temperature profile measurements at all tower levels of 8, 15, 32, 47, 63, 80, 102, 120, 140, 160, 180, 200, 240, 280, 320 m, for five days, October 19 to 23, 1998, which were sampled at a frequency of 3 times per minute. These data were measured by means of Psychrometers and cup-anemometers at northwest and southwest direction. We choose the data in the direction of the northwest according to the prevailing wind direction at that time.

The second data-set, which represents an instantaneous three-component velocities and temperature with sampling frequency of 10 times per second (10 Hz), sampling length of 1 hour, was measured by three dimensional sonic anemometer-thermometer instruments at 47, 140, 280 m levels, during the period of October 14 to 23, 1998.

The instantaneous values of absolute temperature $T(= |\overline{T} + T'|)$ were obtained from the sound speed measurements obtained from the 3-D sonic anemometer by using the following formula, neglecting water vapor fluctuations (Feynman et al., 1963; Kaimal and Finnigan, 1994)

$$c^2 = 403|\overline{T} + T'|(1 + 0.32e/p) , \tag{17}$$

where c is the speed of sound, e is the water vapor pressure and p is the atmospheric pressure. The temperature data obtained from (15) have been compared with those from a fine wire thermocouple instruments and have been applied successfully in the other studies (Albertson et al., 1995; Kiely et al., 1996).

Before spectra and cospectra were computed by using "Fast Fourier Transform (FFT)" the data preprocessing was made, which included that the coordinate system was transferred into mean wind as the X-axis direction, a second order polynomial fit was applied for linear detrending and bell tapering was used at 10% of the beginning and ending of the recording length (Stull, 1988). The aliasing was minimized by low-pass filter with an appropriate cut-off frequency at high wavenumbers.

4. Results and discussion

4.1 *Dimensionless wind and temperature gradients*

4.1.1 *Result for unstable conditions*

The non-dimensional gradients of wind and temperature, Φ_m and Φ_h, evaluated by the three methods mentioned in Section 2, were presented in a wide range of stability parameter $\zeta_1(|\zeta_1|$ up to 10). In order to examine the validity of these results as well as the difference between them and the results reported by Hu and Zhang (1993) and Xu et al. (1997), we plot them against stability parameter together in Figs. 1a and 1b for Φ_m and Φ_h, respectively. The remarks (*), (+) and (•) are the individual measurement points for Φ_m and Φ_h calculated by eddy correlation, mean profile and inertia-subrange cospectra methods, respectively. The results from the various methods have similar trend over the entire stability range, but the points derived by the first method are more scatter than those from the other methods. This scatter is due to the direct calculation of u_{*1} by using (3), which yielded also high scatter for measurements of momentum flux calculated by Al-Jiboori et al. (1999) for the same used data.

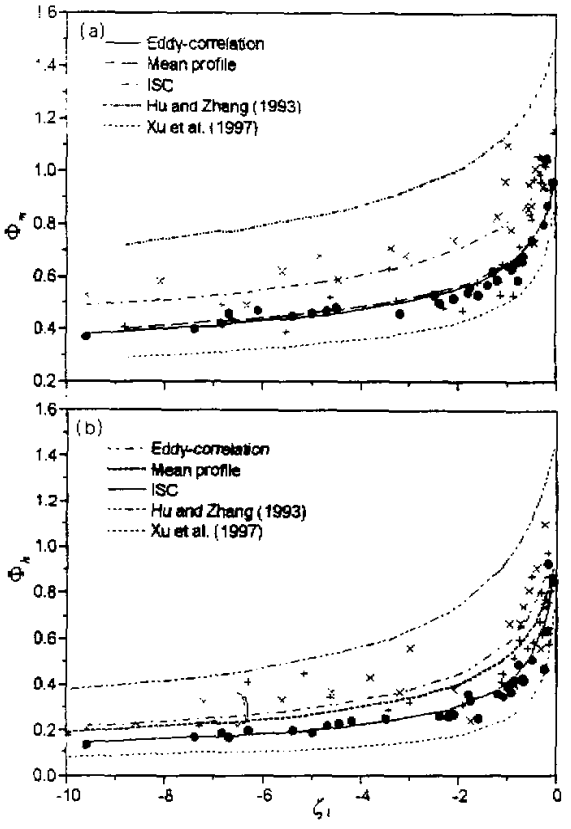

Fig. 1. Non-dimensional gradients of mean wind speed and temperature, Φ_m and Φ_h as a function of ζ_1 under unstable conditions. The symbols ×, + and ○ denote results of eddy-correlation, mean profiles and ISC methods, respectively.

In this study we use the general expressions of Φ_m and Φ_h, respectively

$$\Phi_m = a(1 - b\zeta_1)^{-1/4} \qquad \zeta_1 < 0 \,, \tag{18}$$

$$\Phi_h = a(1 - b\zeta_1)^{-1/2} \qquad \zeta_1 < 0 \,. \tag{19}$$

Each equation contains the empirical constants a and b, which are based on observations but the values of Φ_m and Φ_h are different slightly for observations, with $\alpha = 1.1$, 0.97 and 1.0, and $b = 2.5$, 3.8 for Φ_m and 2.4 for Φ_h, and 4.8 derived from eddy correlation, mean profiles and ISC methods, respectively, while they were 1.5, and 2.0 for Φ_m and 1.5 for Φ_h obtained by Hu and Zhang (1993). Comparing results of the three methods each other and with those reported by Hu and Zhang (1993) and Xu et al. (1997), we can see that all of curves have similar trend near the neutral region, and have apparent separation with the increase of instability, because Φ_m and Φ_h are sensitive to the magnitudes of a and b when $-\zeta_1$ increases. In addition, the curves from last two methods are often close to each other and to results of Xu et al.

(1997) and Carl et al. (1973), but there is a significant difference between them and those from the eddy correlation method, especially for the results of Φ_m.

4.1.2 *Results for stable conditions*

Most studies of mean wind speed and temperature profiles have found that Φ_m and Φ_h were proportional to ζ_1 in the form

$$\Phi_m = \Phi_h = a(1 + b\zeta_1) , \qquad \zeta_1 > 0 \tag{20}$$

The constants a and b were found to be 1.5 and 0.3 by Hu and Zhang (1993) obtained from meteorological tower. Through the fitting of function $\Phi_m (= \Phi_h)$ calculated by the three methods we found that a was 0.8, 0.95 and 0.9, and b was 1.8, 2.7 and 3.6 respectively, which are larger than those given by Hu and Zhang (1993). The values of a and b from mean profile and inertia–subrange cospectra methods are very close to results reported by Xu et al. (1997), because the fluctuation data are also from tower-layer atmosphere. We put all of Φ_m and Φ_h values derived by various methods with the results obtained by Xu et al. (1997) and Hu et al. (1993) into Fig. 2 for comparison.

Figure 2 shows that generally, the scatter of the individual data points for Φ_m and Φ_h under the stable stratifications is much larger than those under the unstable conditions. Because of the larger scatter for a few data points derived by eddy–correlation, the curve fitted seems relatively away from the curves of other methods. In addition, the curve from the eddy correlation method by Xu et al. (1997) is located between the curves of mean profile and cospectra methods, which confirms the validity of results derived by these two methods. Thus, the results of eddy–correlation may be attributed to the direct use of raw data, in contrast the inertia–cospectra method requires some modifications for these data, which was mentioned in Section 3.

4.2 *Average dissipation rate*

In fact, the computation of gradient functions of Φ_m and Φ_h by the ISC method is also the first calculation of the dissipation rates of TKE, Φ_ε. This Φ_ε is important, which is related

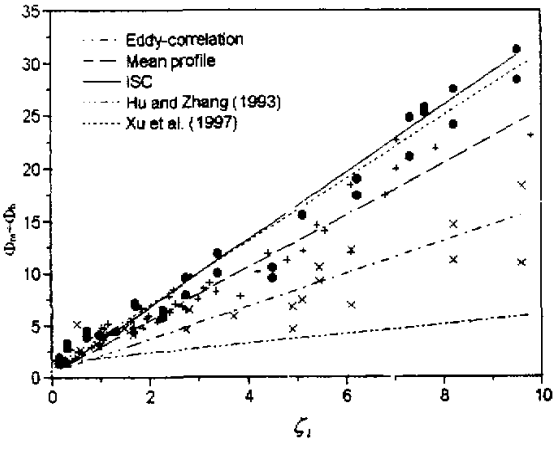

Fig. 2. Same as Fig. 1, but for stable conditions.

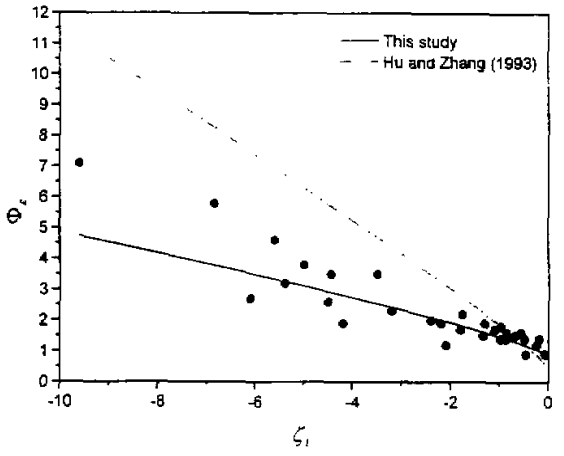

Fig. 3. Non-dimensional dissipation rates for turbulent kinetic energy as a function of ζ_1 under unstable conditions.

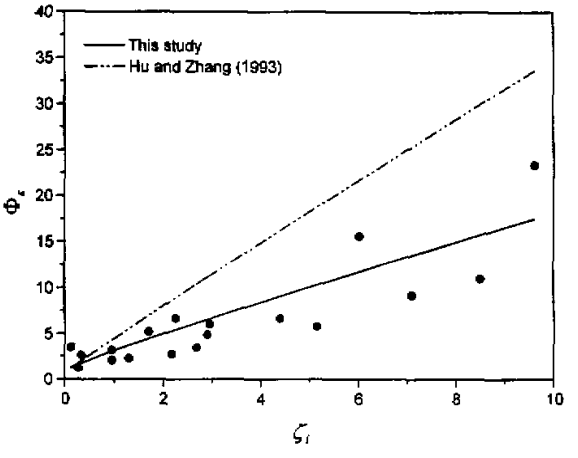

Fig. 4. Same as Fig. 3, but for stable conditions.

to the production rate of TKE through the simplified turbulent kinetic energy budget equation. In this study, however, the normalized dissipation rates, Φ_ε, were computed directly by using the spectral densities of longitudinal velocity under unstable and stable stratifications as the average over a wide range of band-frequency within the region of '$-2/3$' slope in the inertia-subrange. Non-dimensional dissipation rates Φ_ε of power spectra are plotted versus ζ_1 in Figs. 3 and 4 under unstable and stable conditions with early some results of Hu and Zhang (1993) as a reference paper. The general expression can be used to fit dissipation rates data

$$\Phi_\varepsilon = a(1 + b|\zeta_1|^{2/3})^{3/2} \quad . \tag{21}$$

taking Φ_ε to be unity at neutral, where a and b are the empirical constants. In unstable conditions, initially they were found to be smaller than 0.4 and 1.8 reported by Hu and Zhang (1993). The values of 0.8 and 0.5 were obtained by us in this study represented by the solid line.

For the stable conditions, the values of a and b in our study were 0.8 and 1.5, which are also a little smaller than 0.4 and 4.0 suggested by Hu and Zhang (1993). In order to illustrate these differences, the curves fitted were presented in Figs. 3 and 4 under unstable and stable conditions, respectively. We can see that all of these curves go through 1.0 at the origin, but there are apparent differences with the increase of (in−) stability.

4.3 *Ratio of eddy diffusivities*

In application of the mean wind and temperature profiles technique, we calculated the ratio of eddy thermal diffusivity K_h to eddy viscosity K_m, space $\alpha = K_h / K_m$ under stable and unstable conditions. According to (1), (2), (3), (4) and (12), α can be represented as

$$\alpha = \frac{\Phi_m}{\Phi_h} \quad . \tag{22}$$

Then, we transformed stability parameter ζ'_1 to ζ_1 by using (8). This transformation is important to compare results with other methods. There exists considerable uncertainty in variation of α with ζ_1 under unstable and stable conditions in the ABL. The values of α obtained from (22) are shown in Fig. 5 in a wide range of $|\zeta_1|$. As the previous discussion in Section 4.1, the scatter of α on both sides is more than that in Φ_m and Φ_h plots because u^2_{*1} is involved (9). Figure 5 shows that the values of α clearly increase with increasing instability. By substituting (18) and (19) into (23) the following equation represented by the solid line in Fig. 5 is given:

$$\alpha = 1.05(1 - 1.5\zeta_1)^{1/4} \qquad \zeta_1 < 0 \ . \tag{23}$$

It shows clearly that the constant α is 1.05 at $\zeta_1 = 0$, which is very close to 1.0 assumed in

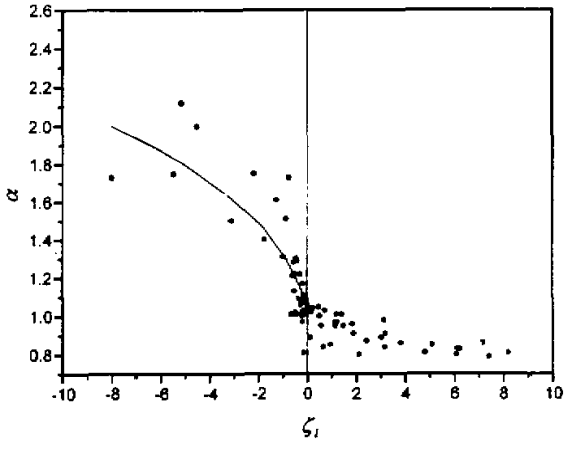

Fig. 5. Ratio of eddy diffusivities, $\alpha (= K_h / K_m)$ as a function of ζ_1 for unstable and stable conditions.

Webb (1970), and less than the value of 1.35 suggested by Businger et al. (1971).

In stable air, α decreases slowly with increasing of ζ_1 (up to 2.0). This behavior is in good agreement with the result obtained by Businger et al. (1971), but it is incompatible with Carl et al. (1973) and Webb (1970). The average value of α goes below unity which is about 0.83 if $\zeta_1 > 2.0$.

4.4 *Normalized spectra and cospectra*

If we now divide the left-hand sides of Eqs. (13), (14) and (16) by the quantities $\Phi_m \Phi_\varepsilon^{1\ 3}$, $\Phi_h \Phi_\varepsilon^{1\ 3}$ and $\Phi_\varepsilon^{2\ 3}$ respectively, we remove the stability dependence in their equations. This brings all cospectra / spectra into coincidence in the inertia-subrange, while the cospectra / spectra peaks will spread out at low-frequency parts according to stability. This form of normalization has been applied to the cospectra / spectra presented in Figs. 6 and 7. These figures display spectral behavior of u, space uw and wT versus non-dimensional frequency f on the log-log plot. However, In order to simplify the analysis of the spectral / cospectral data of this study, the runs were divided into five groups according to stability parameter ζ_1, which ranged from −2.0 to +2.0. The boundaries of each group and their remarks were given in the caption of Fig. 6.

It is clear that the normalized spectra / cospectra reduced to a family of curves, which has been found by Kaimal et al. (1972) and Roth and Oke (1993). In addition, the scatter of cospectral data of uw and wT in the area of low frequency is more than that of u-spectral data. It shows that the actual scatter in Fig. 7 is probably a good measure of any statistical quantity (Pond et al., 1971). We can conclude from our results that using the ISC method in calculating the non-dimensional gradients of Φ_m and Φ_h is a reasonable guide to ensure the validity of cospectra sensitivity measurements.

Figure 6 shows that the u-spectra follow the '−2 / 3' power law in inertia-subrange, according to Kolmogorov law of slope '−5 / 3'. The spectral data cluster of the low frequency appears approximately similar to those given by Kaimal et al. (1972) and Roth and Oke (1993) with a shift of stable spectra peaks towards low frequencies. While the uw- and

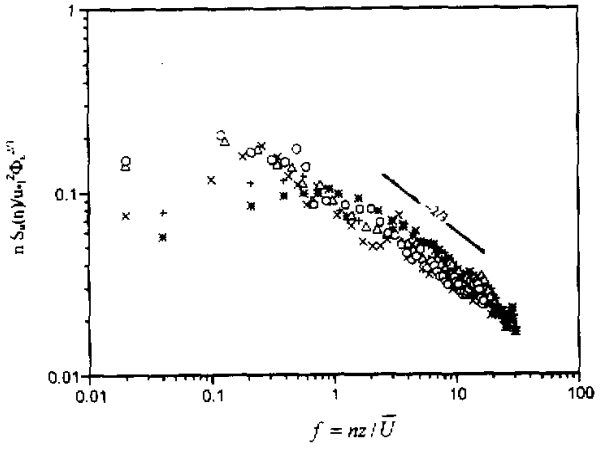

Fig. 6. Normalized u-spectra for five groups versus non-dimensional frequency f. Following remakes represent ranges of ζ_1 value: (*) → $0.5 \leqslant \zeta_1 \leqslant 2.0$, space (+) → $0.11 \leqslant \zeta_1 \leqslant 0.27$, (×) → $0.06 \leqslant -\zeta_1 \leqslant 0.2$, (△) → $0.21 \leqslant -\zeta_1 \leqslant 0.99$ and (○) → $1.0 \leqslant -\zeta_1 \leqslant 2.0$.

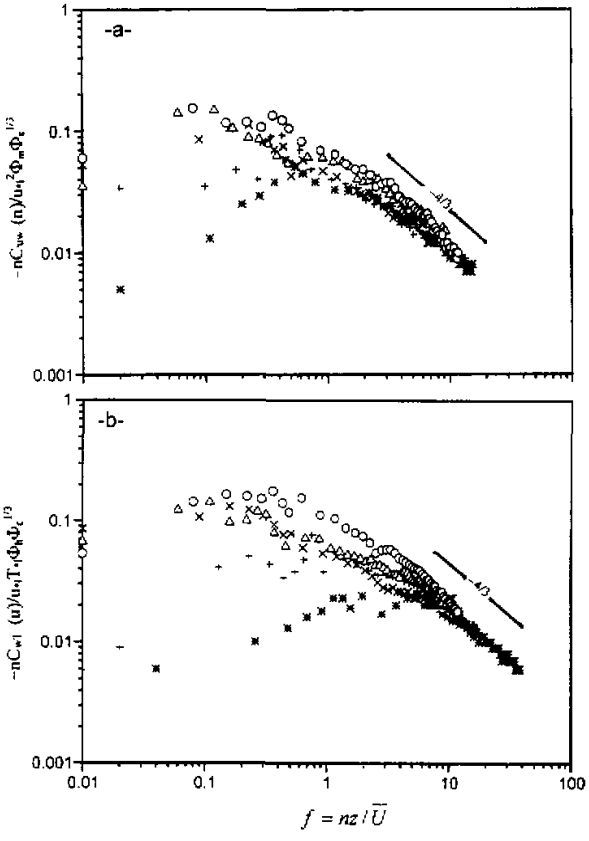

Fig. 7. Same as Fig. 6, but for normalized cospectra (a) uw and (b) wT.

wT–cospectra shown in Fig. 7 follow '$-4/3$' power law which decrease more rapidly with frequency than that for spectra. The results from this study are in good agreement with those from Kaimal data, i.e. uw– and wT–cospectra crowed into a relatively narrow band at the low–frequency end under unstable conditions, while the location of cospectral peaks shifts as a function of ζ_1 in stable air.

5. Concluding remarks

In this study, local similarity scaling was successfully applied to deriving a number of similarity functions of the single parameter z/L_1 for flux–gradients, dissipation rate and ratio of eddy diffusivities. The non–dimensional wind and temperature gradients, Φ_m and Φ_h, were calculated by three techniques: eddy–correlation, profiles of mean wind and temperature and ISC method. The empirical constants obtained by (18), (19) and (20) under the unstable and stable conditions are shown as follows:

Condition	Unstable		Stable	
Method	Empirical constants in (18) and (19)		Empirical constants in (20)	
	a	b	a	b
Eddy-correlation	1.1	0.5	0.8	1.8
Mean profile	0.97	3.8 for (18) 2.4 for (19)	0.95	2.7
ISC	1.0	4.8	0.9	3.6

Because the large scatter of the data points calculated by eddy-correlation as well as its values of a and b differs from last two techniques and others, we found in our study that the results from the mean profiles and ISC approaches are usually close to each other and similar to that from Xu et al. (1997).

The ISC method being of particular features not only shows that its good results with common results, but also provides an extensive insight of study characteristics of ABL. Besides the computation of Φ_m and Φ_u, the dissipation rate for turbulence was calculated by using u-spectra for both unstable and stable conditions.

The ratio of the eddy diffusivities for heat and momentum was estimated to transform ζ'_1 into ζ_1 in the application of mean profiles methods. The ratio is a little greater than 1.0 at neutrality; it shows a marked increase when $\zeta_1 \to -10$, and a slow decrease when $\zeta_1 < 2.0$ and then more constancy appears at $\zeta_1 > 2.0$.

The authors are very grateful to the members, working for the State Key Lab. of Atmospheric Boundary Layer Physics and Atmospheric Chemistry, the Institute of Atmospheric Physics in Beijing, who supplied the data from the meteorological tower for this paper. The authors wish to thank to Mrs. Israa H. A. in the presentation of data on the required style.

REFERENCES

Albertson, J. D., M. B. Parlange, G. G. Katul, C. R. Chu, H. Stricker, and S. Tyler, 1995: Sensible heat flux from arid regions: A simple flux-variance method. *Water Resource Res.*, **31**, 969-973.

Al-Jiboori, M. H., Xu Yumao, and Qian Yongfu, 1999: Diurnal variation of turbulent fluxes in tower-layer atmosphere. In workshop on meso-scale systems in meiyu / bain front and hydrological cycle, Game / Hubex project office, Xi'an, China, 110-113.

Al-Jiboori, M. H., Xu Yumao, Qian Yongfu, 2000: Local similarity relationships and average dissipate rate of turbulence in the tower-layer atmosphere. Submitted to *Bound.-Layer Meteor.*

Antonia, R. A., A. J. Chambers, D. Phong-Anant., and S. Rajagopalan, 1979: Properties of spatial temperature derivatives in the atmospheric surface layer. *Bound.-Layer Meteor.*, **17**, 101-118.

Businger, J. A., J. C. Wyngaard, Y. Izumi, and E. F. Bradley, 1971: Flux-profile relationships in the atmospheric surface layer. *J. Atmos. Sci.*, **28**, 181-189.

Carl, D. M., T. C. Tarbell, and H. A. Panofsky, 1973: Profiles of wind and temperature from towers over homogeneous terrain. *J. Atmos. Sci.*, **30**, 788-794.

Feynman, R. P., R. B. Leighton, and M. Sands, 1963: *The Feynman Lectures on Physics*, Vol. 1, Addison-Wesley, 47 pp.

Hu Yinqiao, and Zhang Qiang, 1993: On local similarity of the atmospheric boundary layer. *Scientia Atmospherica Sinica*, **17**, 10-20 (in Chinese).

Kaimal, J. C., and J. J. Finnigan, 1994: *Atmospheric Boundary Layer Flows. Their Structure and Measurement*. Oxford University Press, 289 pp.

Kaimal, J. C., J. C. Wyngaard, Y. Izumi, and O. R. Cote, 1972: Spectra characteristics of surface-layer turbulence. *Quart. J. Roy. Meteor. Soc.*, **98**, 563-589.

Kiely, G., J. D. Albertson, M. B. Parlange, and W. E. Eichinger, 1996: Convective scaling of the average dissipation rate of temperature variance in the atmospheric boundary layer. *Bound.-Layer Meteor.*, **77**, 267–284.

Monin, A. S., and A. M. Obukhov, 1954: Basic laws of turbulent mixing in the atmospherie near the ground. Tr. Akad Nauk. SSSR Geophiz. Inst., **24(151)**, 1963–1987.

Nieuwstadt, F. T. M., 1984: The turbulent structure of the stable, nocturnal boundary layer. *J. Atmo. Sci.*, **41**, 2202–2216.

Pond, S., G. T. Phelps, J. E. Paquin, G. McBean, and R. W. Stewart, 1971: Measurements of the turbulent fluxes of momentum, moisture and sensible heat over the ocean. *J. Atmos. Sci.*, **28**, 901–917.

Roth, M., and T. R. Oke, 1993: Turbulent transfer relationships over an urban surface. I: Spectra characteristics. *Quart. J. Roy. Meteor. Soc.*, **119**, 1071–1104.

Sorbjan, Z., 1986a: On similarity in the atmospheric boundary layer. *Bound.-Layer Meteor.*, **34**, 377–397.

Sorbjan, Z., 1986b: Local similarity of spectral and cospectral characteristics in the stable-continuous boundary layer. *Bound.-Layer Meteor.*, **35**, 257–275.

Stull, R. B., 1988: *In Introduction to Boundary Layer Meteorology*. Kluwer Academic Publishers, Dordrecht 308 pp..

Sugita, M., T. Hiyama, N. Endo and S. Tian, 1995: Flux determination over a smooth surface under strongly unstable conditions. *Bound-Layer Meteor.*, **73** 145–158.

Webb, E. K., 1970: Profile relationships: The log-linear range, and extension to strong stability. *Quart. J. Roy. Meteor. Soc.*, **96**, 67–90.

Wyngaard, J. C., and O. R. Cote, 1972: Cospectra similarity in the atmospheric surface layer. Quart. *J. Roy. Meteor. Soc.* **98**, 590–603.

Xu Yumao, Zhou Chaofu, and Li Zongkai, 1997: Turbulent structure and local similarity in the tower layer over the Nanjing Area. *Bound.-Layer Meteor.*, **82**, 1–21.

Yin Dazhang, and Hong Zhongxiang, 1999: Study on the boundary layer structure and parameter under heavy pollution condutions in Beijing. *Climatic. Environ. Res.*, **4**, 303–307 (in Chinese).

Zhang Aichen, Lu Jie, Zhang Bing, and Liu Shuhua, 1991: The turbulence characteristics in the boundary layer of the rural area and border of urban area of Beijing. *Scientia Atmospherica Sinica*, **15(4)**, 87–96 (in Chinese).